Spray Plume Characteristics at Multiple Cross-Flow Angles, Experimental and Computational Assessments

K. M. Bade*, W. Kalata, and R. J. Schick
Spray Analysis and Research Services
Spraying Systems Co.
P.O. Box 7900
Wheaton, IL 60187 USA

Abstract

The interaction of a spray plume within a confined cross-flow environment occurs often in spray applications, most notably in gas conditioning applications. Characterization and modeling of the drop size and velocity distributions, as well as spray shape, was conducted within a controlled wind tunnel environment. The primary focus of this study is the effect of various incident angle cross-flows on the characteristics of a spray nozzle.

While the spray characteristics immediately downstream of the nozzle will govern the significance of the effect of the cross-flow, this study aims to provide a reference case in order to guide and compare future work. A low flow rate, hydraulic, hollow cone spray was investigated with a nominally uniform cross-flow air speed of 15.4 m/s. These results demonstrate the trajectory change as well as the change in spray plume characteristics over a range of spray angles defined relative to a co-flow air stream.

The experimental results were acquired with an Artium Phase Doppler Interferometer (PDI). The computational model and simulations were conducted using the Ansys Fluent modeling software package in conjunction with methods developed at Spraying Systems Co. The computational model's agreement, and disagreement, with the experimentally acquired results provides insight for the appropriate considerations when constructing cross-flow models.

Introduction

Process improvement and optimization in the gas conditioning industry is a constantly ongoing effort. The improvements made in nozzle design and liquid atomization in recent years have provided the possibility of process optimization like never before. While on-site experimental testing provides the most direct assessment of a spray's characteristics in a gas conditioning tower, often the cost and availability of these tests is limited or impossible. Therefore, computational fluid dynamics (CFD) projects for this type of application have become very useful. With CFD, gas conditioning process engineers are able to, for the first time, assess the spray quality within the *actual* spray process region. The increased use of CFD to model these processes requires in-depth validation of the methods used to model these applications and the results provided by these types of models.

Spraying Systems Co. has the unique combination of testing and modeling expertise that allowed for a rigorous validation of these modeling techniques often used to simulate *un-testable* situations. This validation of computation fluid dynamics (CFD) results is wide reaching in applicable variables; the focus of the present study was on the relative angle of the spray nozzle to a steady, nominally uniform co/cross-flow air stream. Orientation angles of the spray nozzle axis (α) varied from 0° (in-line with the co-flow air) to 90°; at 15° intervals for testing; and at 45° intervals for modeling.

Equipment and Methods

Experimental Setup and Methods

The experimental setup consisted of a spray nozzle, wind tunnel, and Artium Technologies Phase Doppler Interferometry system (PDI). All tests were carried out with the cross-flow air and spray liquid at ambient temperature ~68°F. The nozzle was operated with a steady 3.8 bar (55psi) clean water supply for all tests.

*Corresponding author

Wind Tunnel

The wind tunnel utilized in these experiments was capable of producing nominally uniform air flow at a velocity range from 2.5 m/s to greater than 50 m/s; the actual co/cross-flow velocity generated during these tests was 15.4 m/s. This wind speed was chosen as it allowed for a *reasonable* amount of deflection of the spray plume within the first 600mm (location of wind tunnel optical access) of the spray injection.

Phase Doppler Interferometry

The phase Doppler Interferometry system used in this study was the Artium PDI 2D MD instrument with the integrated AIMS software used for automated processor setup. This technique measures the size, velocity, angle of trajectory, and time of arrival of each particle passing through an optical measurement volume formed by pairs of intersecting laser beams. The technical explanation of the Phase Doppler technique can be reviewed in a number of publications including Bachalo and Houser [1] and Bachalo 1985 [2]. The ability to measure accurately requires the reliable characterization of the size, velocity, and transit time of each droplet. The PDI system is a validated method for droplet size and velocity measurement; in addition, spray concentration measurements are possible, see Bade [3].

The Artium PDI system utilizes a unique digital signal burst detection method which reliably detects droplets, even in complex environments. This is an advance over the earlier Fourier transform burst detection method invented by Ibrahim and Bachalo (U.S. Patent 5,289,391). This detection system is also critical to the in situ approach for measuring the effective diameter of the sample volume as a function of drop size. The Fourier transform based signal processor uses quadrature down-mixing to position the signals in an optimum range for processing. The real and imaginary (shifted by 90 degrees) components of the signals are sampled and a full complex Fourier transform is used to obtain the signal frequency and phase. Each of the three signals for the phase measurements is sampled in this manner and the phase differences computed at the same frequency for each signal. Three phase differences are computed, AB, AC, and BC for detectors A, B, and C from the Channel1 velocity component. These three phase differences are compared for consistency as one of the validations for each droplet signal detected. The approach has proven to be very effective in detecting and eliminating sizing errors due to the well-known trajectory problem.

The Artium AIMS software incorporates an *auto-setup* feature that serves to optimize the frequency and phase shift processing. The auto-setup feature acquires a small number of signals produced by droplets passing through the measurement volume and is discussed in detail in Bachalo, et al. [patent pending]. User-to-user setup differences that have been known to produce varying results and accuracy in PDI data results, often relying upon the operator's individual experience and understanding of the PDI principals, have been significantly minimized with this approach. The laser transmitting lens focal length was 1000mm for all tests; the receiving unit focal length was 500mm for all tests and was oriented at the 40° off-axis forward scatter position. This provided an effective measureable drop size range of 2.3 to 282μm. Fig. 1A demonstrates the wind tunnel experimental setup with a PDPA setup mounted around the wind tunnel test section, for these tests, an Artium PDI was setup in a similar manner.

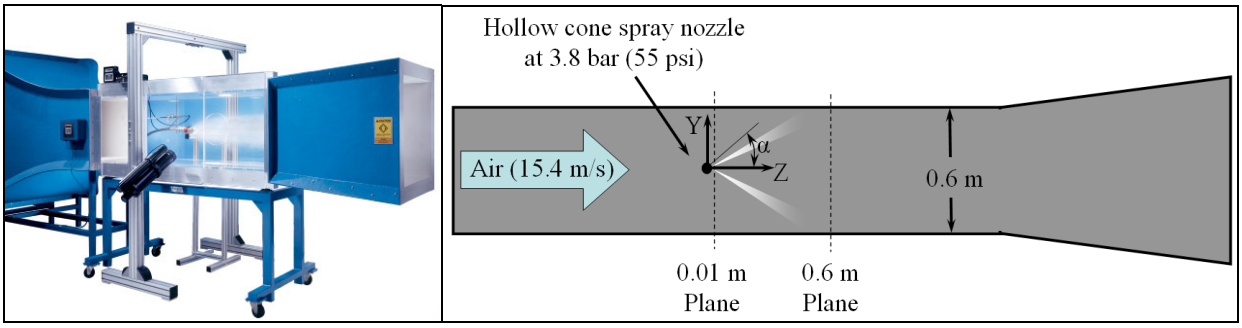

A **B**

Figure 1. A. PDPA mounted with wind tunnel **B.** Wind tunnel geometry

Computational Setup and Methods

CFD simulations were performed with ANSYS FLUENT version 6.3. Generally, the CFD model was reproduced according to the wind tunnel geometry. The most significant alteration in the modeled geometry was the spray lance which was simplified to reduce the upstream mesh size. Meshing was performed within GAMBIT 2.4. Dense mesh was incorporated in the near vicinity of the spray injection locations. Size functions were used to further reduce mesh size. The 3D mesh consisted of mixed elements with approximately 1.3 million cells. Figure 1B provides

a two-dimensional schematic of the CFD model setup and defines the coordinate system referenced in both the computational and experimental results.

The CFD model was set up with a uniform velocity inlet boundary condition (BC) while varying the relative spray injection incident angle, relative to the axial air flow direction (α = 0° [co-flow], 45°, and 90° [cross-flow]). The outlet side of the duct was defined with a constant pressure boundary condition. The Tunnel duct and lance walls were specified as rigid with no-slip and adiabatic conditions. Throughout all simulations the following models were included: k-ε Realizable Turbulence Model, DPM for LaGrangian tracking of water droplets, and Species Transport Model to include mixing of air and water vapor due to evaporation. The air phase and particle tracking were performed in steady state.

$$Q = 1 - \exp\left(-\frac{D}{X}\right)^{q} \qquad (1)$$

The drop size distributions, velocity (13.3 m/s), and spray plume angle (90º) were obtained while conducting the PDI measurements and used to define the CFD model spray injection parameters. The iInjection velocity was based on volume flux and area weighted averaged velocity at 10 mm downstream from the nozzle exit orifice, these weighing techniques are discussed in Bade [4]. These initial spray characteristics were acquired with the wind tunnel in operation using the PDI system describe previously. The drop size range that was used to specify spray injections in FLUENT was derived from a combination of the x=10 mm and x=600 mm locations. The minimum diameter (22 µm) input for CFD was specified based on volume flux and area weighted average of $D_{V0.01}$ [5] and [6] from the profile at 10 mm from injection. The maximum diameter (220 µm) for the CFD model was specified based on volume flux and area weighted average of $D_{V0.99}$ at the z=600mm downstream location. This process of combining the initial drop size characteristics and downstream characteristics was necessary in order to account for the lack of droplet collision and coalescence in the model. The injection volumetric mean diameter (108 µm) for CFD was determined based on volume flux and area weighted averages of $D_{V0.5}$ from both locations. The FLUENT input for drop size distribution was specified using the Rosin-Rammler distribution function, see Equation 1, to account for the 20,000 particles that were tracked at each iteration of the DPM model [6]. Q is the fraction of total volume of drops with diameter less than D. X and q are constants inherent to the Rosin-Rammler function associated with the distribution center and width, respectively. The user-defined function was used to calculate SMD [5] while running 50 iterations after resolving the flow field.

Results and Discussion

The experimental results are presented for two downstream distances. First, the spray characteristics are examined at 10mm downstream from the nozzle exit orifice (z=10mm). At this distance, all results were acquired with the nozzle spraying in a purely co-flow orientation (angle=0°).

Downstream Distance: 10mm

The results at the downstream location z=10mm are provided in order to show the initial characteristics of the spray plume upon exiting the nozzle. Figures 2 and 3 provide the D32 and Axial Velocity profiles, respectively, with the wind tunnel in operation (15.4 m/s) and also when not in operation.

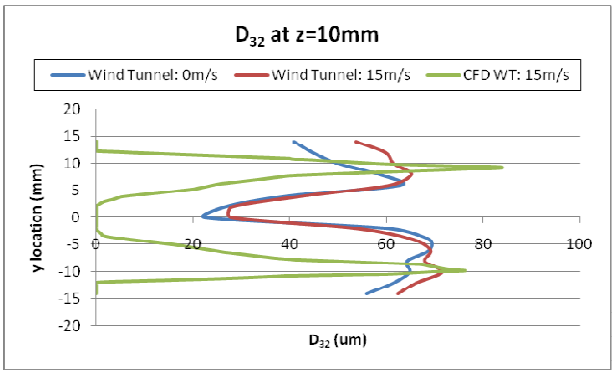

Figure 2. D_{32} results at z=10mm

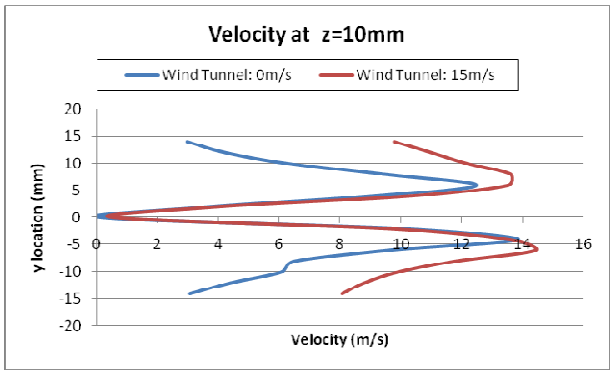

Figure 3. Axial Velocity results at z=10mm

As expected, the drop size is similar with and without the co-flow air in operation. However, with the co-flow air *on*, many of the smaller particles do not possess sufficient momentum, after exiting the nozzle, to maintain their initial trajectory (and overcome the drag caused by the co-flow air stream) and continue to move outward from the nozzle centerline. Thus, the D_{32} values at y < 5mm (inside of hollow cone) remain nearly identical with and without the wind tunnel, while the D_{32} values at y > 5mm (outside of hollow cone) increase by approximately 5-20%. In addition to the reduced count of small droplets in the y>5mm, the zero velocity spray environment may cause additional breakup of the largest droplets in the outside region due to shear on the droplets surfaces.

The difference on the *inside* and *outside* of the hollow cone profiles are also seen in the axial velocity results. As with the D_{32} results, the velocity values at y < 5mm are very similar with and without the wind tunnel in operation. The y > 5mm region exhibits a much higher velocity with the wind tunnel in operation. This is clearly due to the co-flow air stream that is maintaining the droplet velocities, and perhaps even accelerating the drop velocities due to the slightly higher wind tunnel velocity (15.4 m/s) than the initial droplet axial velocity (13.3 m/s).

PDI at Downstream Distance: z=600mm

The drop size and velocity results at the z=600mm location provide good incite to the effects of various cross-flow angles. Figures 4 and 5 provide the PDI results at this downstream location.

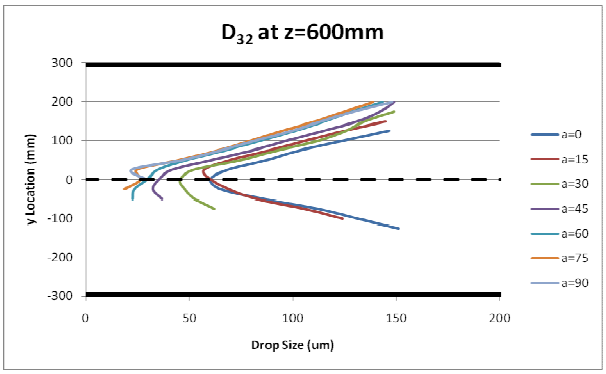

Figure 4. D_{32} results at z=600mm

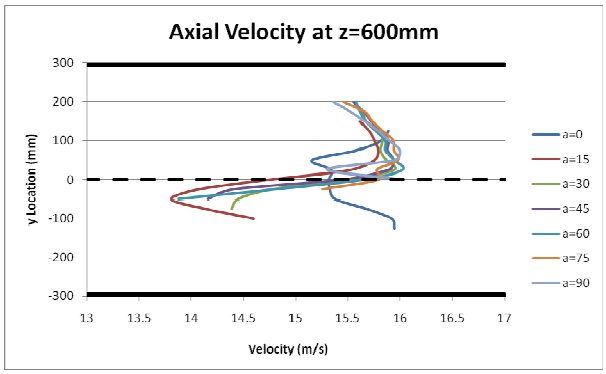

Figure 5. Axial Velocity results at z=600mm

In Figure 4, the effect of various nozzle angles (relative to the purely axial cross stream air flow) on the D_{32} distribution results are demonstrated. As the nozzle orientation angle is increased, the D_{32} values decrease at each positive y-location from the wind tunnel centerline (y=0). For each incident angle, the D_{32} values increase as the distance from the nozzle (and wind tunnel) centerline is increased. This trend follows the expected results due to the larger (higher momentum) particles being sprayed at increasingly larger incident angles. The extents of the data (-100<y<+200mm) for both drop size and velocity testing results was set according to the existence of sufficient droplet concentrations (counts) to allow for *reasonable* data rates with the PDI; as the nozzle incident angle increased. this measureable region moved toward the positive y-direction

Figure 5 demonstrates the change in velocity profile as the nozzle angle is increased. The zero angle (purely co-flow orientation) velocity profile demonstrates the nominally symmetric profile about the wind tunnel centerline. The most notable characteristic is the relatively small change in droplet velocity profiles as the angle is increased from 30° to 90°. The minimum velocities in Figure 5 are very near the droplet injection velocity of 13.3 m/s, whereas the highest velocities in Figure 6 are 3.9% higher than the air stream velocity of 15.4 m/s. This slight increase makes sense due to the spray angle, as the nozzle is angled, the injection begins to align with the wind tunnel axial direction (z) and therefore the initial droplet *axial velocity component* will effectively increase.

CFD at Downstream Distance: z=600mm (3D)

Finally, the results from the CFD three-dimensional simulations are provided in order to show the distributions of drop size and velocity as well as the simulated trajectory of the droplets as they interact with the cross-flow air stream. The collapse of the spray plume at the 0° angle, or reduction in spray angle, demonstrates the effects of drag even when the primary droplet velocity is co-current with the surrounding air stream. Additionally, this effect is much more dramatic with the 45 and 90 results which show the relatively aggressive change in droplet trajectory due to the cross-flow air. Figure 6 provides the droplet trajectories as well as the axial velocity (by color). The air stream velocity contour is included at the z=600mm plane.

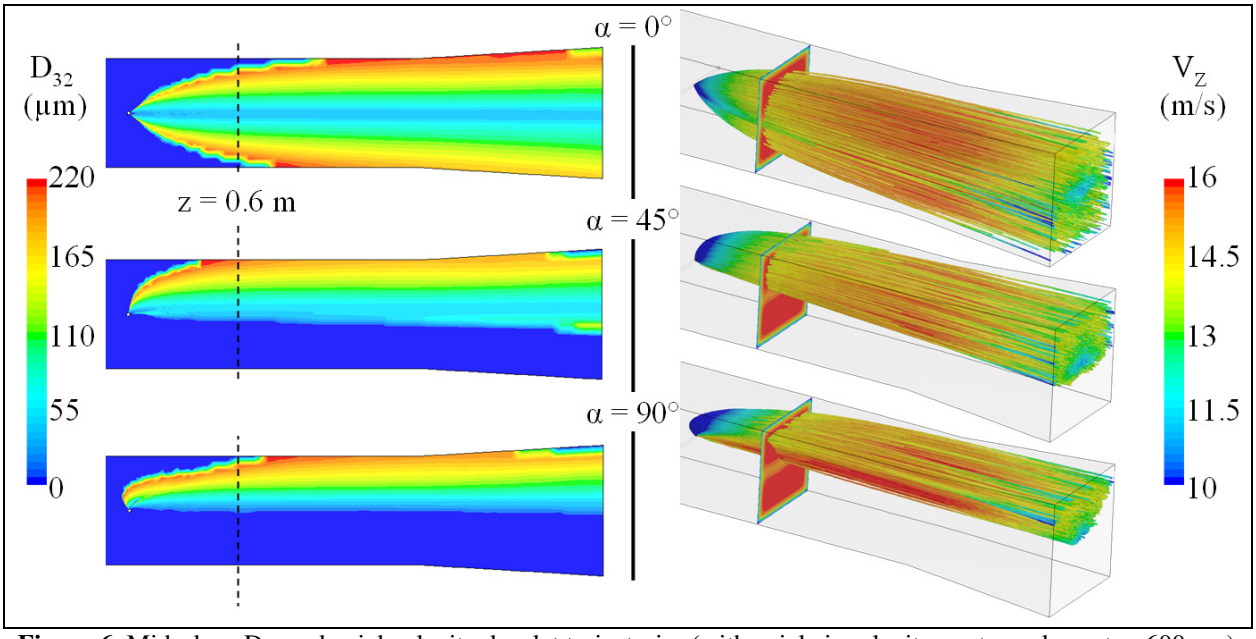

Figure 6. Mid-plane D_{32} and axial velocity droplet trajectories (with axial air velocity contour plane at z=600mm)

Figure 6 demonstrates results of D_{32} and velocity results obtained from the CFD simulations. The notable change in spray plume distribution with an increase in spray angle is demonstrated in the centerline D_{32} contour results of Figure 6. The spray plume *top* edge is oriented with the highest y-direction velocity at the α=45°, this provides the reasonable, but expected result, of a top wall wetting occurring at the most upstream location at α=45°. The z-direction velocity distributions in Figure 6 demonstrate that the spray droplet continue to accelerate downstream of z=600mm until reaching the diverging wind tunnel section. The three-dimensionally resolved simulations were interrogated to provide drop size data at z=10mm and z=600mm to provide direct comparison with the PDI results.

Comparisons and Conclusions

The comparison of PDI and CFD results at z=600mm shows fairly good agreement; however, the D_{32} results differ by approximately 16%. Figure 7 provides the D_{32} profiles at 0°, 45°, and 90° form the PDI and CFD data.

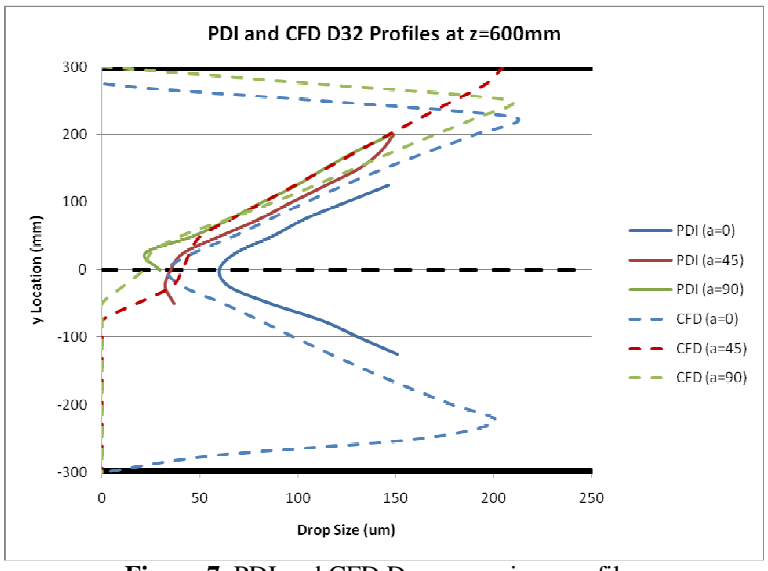

Figure 7. PDI and CFD D_{32} comparison profiles

The Figure 7 results demonstrate the good agreement between the PDI experimental testing data and the CFD modeled data. The primary cause of these apparent differences is mostly likely due to the validity of the input drop size distributions. Differences between the spray plume liquid distribution from the PDI and CFD cases, demonstrated in Figure 2, are mostly likely extrapolated downstream. In Figure 2 the very localized droplet distribution is in contrast to the wider (in the y-direction) distribution of liquid shown in the PDI results.

In terms of the droplet trajectories, the wall wetting distance (on the upper wind tunnel surface) was measured both in the actual wind tunnel as well as in the CFD simulations. This downstream distance is plotted versus spray nozzle angle in Figure 8.

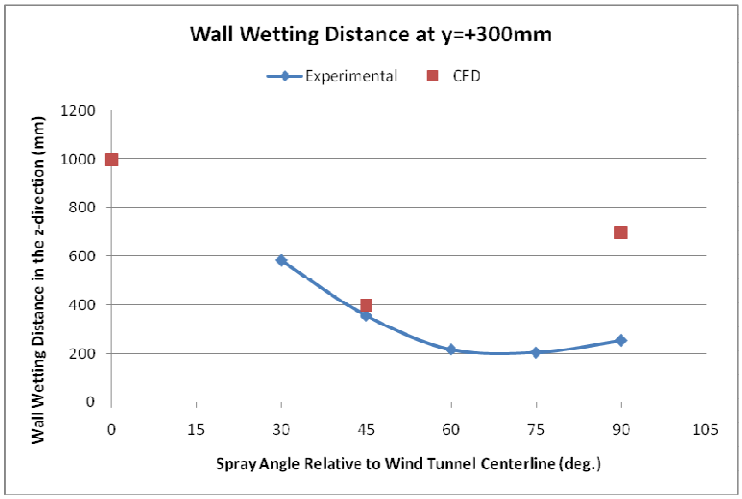

Figure 8. Top Wall (y=+300mm) Wetting Distance, in the z-direction.

The results from the wall wetting distance show very good agreement at the 45 degree angle case; the disagreement at 90° incident spray angle (pure cross-flow) demonstrate the difficulty in accurately modeling a cross flow environment. The disagreement appears to arise due the backward initial trajectory of the particles in the model and will be the focus of future refinement efforts. A possible explanation may focus on the deformation of droplets due to the increased relative velocity of the air stream relative to the drops in addition to additional initial droplet breakup at the near spray injection location. It is encouraging that the experimentally acquired wall wetting distance did begin to increase from 75° to 90° which may indicate that simple refinement of the CFD methods will provie a much more accurate solution. The CFD results at 0° appear to follow the expected trend of the experimentally acquired results.

The experimental and computational results presented here demonstrate the good (droplet trajectory) capabilities of these methods from 0-45° and the good (droplet size) agreements over a much broader range of 0-90°. With the eventual implementation of droplet breakup and coalesce modeling methods, the combined simulation of droplet trajectory and droplet formation CFD will provide more conclusive results. However, the results that are presented were acquired (or generated) using completely from inherently different investigation techniques, namely experimental and computational methods, and the agreement that is shown is quite good.

References

1. Bachalo, W.D. and Houser, M.J., “Phase Doppler Spray Analyzer for Simultaneous Measurements of Drop Size and Velocity Distributions,” Optical Engineering, Volume 23, Number 5, September-October, 1984.
2. Bachalo, W.D. and Houser, M.J., "Spray Drop Size and Velocity Measurements Using the Phase/Doppler Particle Analyzer", Proceedings of the ICLASS (3rd Intl.), July 1985.
3. Bade, K.M., Schick, R.J., “Phase Doppler Interferometry Volume Flux Calculation Optimization and Comparison with Nominally Point Mechanical Patternation Techniques”, ICLASS Intn. 2009, Vail, CO, July 2009.
4. Bade, K.M., Schick, R.J., “Volume Distribution Comparison Methods for 1D, 2D, and Point Measurement Techniques”, ILASS Americas 2008, Orlando, FL, May 2008.
5. Lefebvre, A. H., *Atomization and Sprays*, Hemisphere, New York, 1989.
6. Brown, K., Kalata, W., Schick, R.J.,” Drop Size Distribution Analysis with respect to Height - Numerical Simulation versus Empirical Evaluation”, Proceedings of ILASS 2008, May, 2008.